Check for updates

Proceedings of the ASME 2018
Dynamic Systems and Control Conference
DSCC2018
September 30-October 3, 2018, Atlanta, Georgia, USA

DSCC2018-9198

Downloaded from http://asmedigitalcollection.asme.org/DSCC/proceedings-pdf/DSCC2018/51890/V001T12A002/2376481/v001t12a002-dscc2018-9198.pdf by Georgia Institute of Technology user on 10 August 2020

DESIGN AND VALIDATION OF A TORQUE CONTROLLABLE HIP EXOSKELETON FOR WALKING ASSISTANCE

Inseung Kang, Hsiang Hsu, Aaron J Young PhD
Department of Mechanical Engineering
Georgia Institute of Technology
Atlanta, GA 30332, USA
Email: ikang7@gatech.edu

ABSTRACT

Recent technological advancements have expanded the field of human augmentation. Specifically, lower limb exoskeletons have benefited many by providing assistance to increase mobility. The proposed study aims to develop a novel bilateral hip exoskeleton that provides mechanical power assistance in both hip flexion and extension during walking. Each actuation unit employs series elastic actuator for a high fidelity closed loop torque control utilizing a ball screw transmission incorporated with a fiberglass leaf spring. The control architecture was divided into three tiers and each tier implemented different control algorithms. The device was experimentally validated with both benchtop and human testing. Benchtop testing was done to tune required control parameters in the low-level controller and to validate the torque response. We tested five able-bodied subjects walking with our device. We analyzed their kinematic and kinetic data with different levels of mechanical power assistance during walking. Our benchtop testing results showed that the low-level PID gains were tuned to achieve desired bandwidth and torque tracking. Human testing results demonstrated that the high-level controller provided an accurate information for assistance onset timing that the hip exoskeleton was able to assist the user effectively.

INTRODUCTION

Exoskeleton technology has been introduced and extensively studied over the past years for its significance in broader impact in different fields. Several exoskeletons have been introduced in industry and military applications to augment able-bodied individuals to enhance physical strengths. For example, factory workers use exoskeletons to alleviate work load in lifting heavy objects [1, 2]. Also, exoskeletons have been introduced in military applications for assisting soldiers carrying heavy loads while walking over large distances [3, 4]. Exoskeletons can also be used in healthcare settings as an assistive device for patients with disabilities such as stroke, spinal cord injury, and muscle weakness. Patients using an exoskeleton can not only regain mobility but also benefit in rehabilitation effects from long term usage [5, 6]. Exoskeletons such as Indego [7], ReWalk [8], and Ekso [9] have been introduced in the commercial market for these medical applications to assist patients to regain their mobility in lower limb movement.

Exoskeletons are often complex devices that include multiple powered joints at the hip, knee, and/or ankle. However, while these devices offer potential benefits to disabled populations, the majority of these devices were developed for patients with complete immobility which may not be optimal for other populations. Additionally, these exoskeletons are often operated at slow speeds which may limit community ambulation. Accordingly, such devices are often not applicable to patients who have partial mobility, which is a far bigger segment of the population, including elderly, stroke survivors, children with cerebral palsy, muscular dystrophy patients, and individuals with physical lower limb injuries. To assist such patient populations, it is critical to understand more in depth how to interact with the user biomechanically and effectively deliver power to best restore mobility. To accomplish these tasks, simpler devices which targets a single joint, such as the hip joint, are ideal.

Literature studies have shown that the joint mechanical work produced by the muscles surrounding the hip are the largest contributors to metabolic energy expenditure in human walking [10, 11]. While the ankle joint may contribute large of positive mechanical output, this is mainly done with efficient energy translation (up to 58% energy consumption) with utilizing muscle tendon unit [12]. However, the hip joint, while providing similar magnitude of mechanical power (approximately 45%) as the ankle joint, is not efficient through tendon storage and therefore relies heavily on muscle contribution. For these reasons, providing hip joint assistance during walking may

Copyright © 2018 ASME

benefit more than other lower limb joints metabolically. Additionally, adding mass distal on the leg increases the user's leg inertia, which can be of a greater penalty in terms of energetic cost compared to that of hip exoskeleton which locates the device mass proximal to user's center of mass [13]. These potential hip exoskeleton advantages suits well in its purpose of being used daily in community ambulation.

Recently, several industries and research groups started focusing and developing single joint actuated hip exoskeletons [14-18]. These hip exoskeletons utilize different mechanisms for their actuators such as a harmonic drive gear transmission coupled with a torsional spring for torque measurement [14], a Bowden cable driven soft exoskeleton [15], and a multi-stage gear transmission operating with an open loop control [16]. These devices chose their actuators carefully to maximize the device performance when using different controllers to provide assistance to the user. While the majority of hip exoskeletons were developed with the intention of assisting patients, they have reduced the metabolic rate in able-bodied human walking [16, 19]. While it is exciting to see these exoskeletons bring new platforms for exploring how to effectively assist users during walking, there is a big gap in the research field to fully understand the optimal assistance from the perspective of both human and the robot. Also, some of these devices are only capable of proving small torque magnitudes which may limit to fully comprehend wide range of dynamic motion that human experiences during walking.

We developed a torque controllable bilateral hip exoskeleton to assist humans during walking. This is a testbed system to implement different controllers to understand how to deliver sagittal plane mechanical power to the hip joint to induce the best biomechanical and clinical outcome measures. The design utilizes a set of series elastic actuators using a fiberglass leaf spring incorporated with a gear reduction using a ball screw transmission. Low-level control using these actuators allowed a high fidelity closed-loop torque control to assist the user with known mechanical energy during walking. A high-level control scheme was set to estimate the user's gait phase in real time using gait phase estimator to understand when and how much to provide assistance. Finally, the device was validated both with benchtop testing and five able-bodied subjects walking on a treadmill.

1 MECHATRONIC DESIGN

The exoskeleton is equipped with a set of series elastic actuators (SEAs) at the hip joint for power assistance within the sagittal plane (Fig. 1). The device allows 100° and 30° hip flexion and extension respectively. Additionally, a passive hinge was placed at the hip joint for free motion in both ab/adduction with 15° each along the frontal plane. The device employs three different interfaces for the user: custom made thigh shells, an orthotic pelvic band (Newport 3, Orthomerica, USA), and a shoulder strap. The pelvic band was attached to an additional back plate made of polypropylene fitted to the user from three distinct attachment points (two plates from the side and one from the back) mounted to a carbon fiber frame. The frame and the thigh shells had an adjustable mechanism in size to accommodate different body size (dimension based on accommodating 10% female to 90% male body sizes in the United States [20]). A thigh shell was custom made with carbon infused polycarbonate material for its advantage in high strength in withstanding shear stress exerted by the exoskeleton. Backpack unit comprises all the electronics such as a single board computer, a battery, and a custom circuit board. Although each actuator has a mass of only 1.5 kg each, the entire device (including the battery) has a mass of 7 kg due to increased weight from both pelvic band and thigh shells as they had aluminum metal plates along the attachment point to provide more solid fixture. This weight can be reduced greatly with additional design iterations in the custom interface.

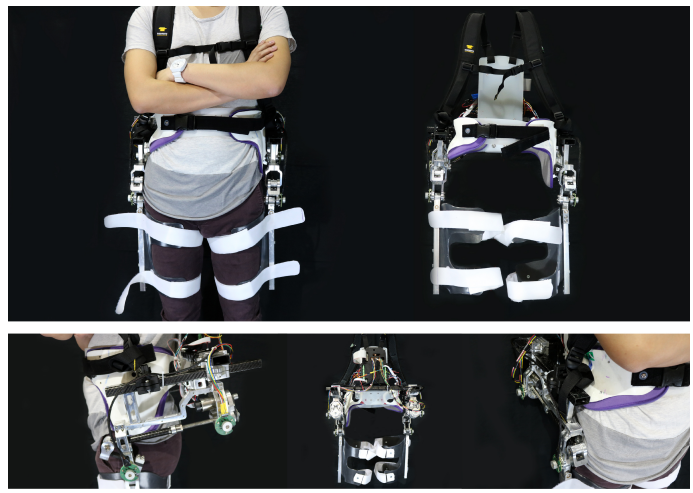

Figure 1. Overview of the torque controllable hip exoskeleton. The figure shows an example of exoskeleton being fitted to the user. The shoulder straps, pelvic band, and thigh shells can be adjusted to accommodate different body sizes.

Main aspects of the device specification are the torque output and angular velocity of the actuator (Table 1). All of the required specification were based on human walking biomechanics. Using the Winter dataset [21], desired torque trajectory and angular velocity over a single gait cycle was analyzed. Human biomechanical data showed that the peak torque at the hip joint during normal walking speed of 1.35 m/s is approximately 0.8 Nm/kg with a maximum velocity of 180 °/sec.

Table 1. Hip exoskeleton device specification

Peak Torque	60 Nm
Rated Torque (Max Cont.)	30 Nm
Maximum Angular Velocity	180 °/sec
Torque Bandwidth	5 Hz
Actuator Weight	1.5 kg
Total Device Weight (Including the Battery)	7 kg
Range of Motion	130° Sagittal Plane 30° Frontal Plane (Passive)

Downloaded from http://asmedigitalcollection.asme.org/DSCC/proceedings-pdf/DSCC2018/51890/V001T12A002/2376481/v001t12a002-dscc2018-9198.pdf by Georgia Institute of Technology user on 10 August 2020

Copyright © 2018 ASME

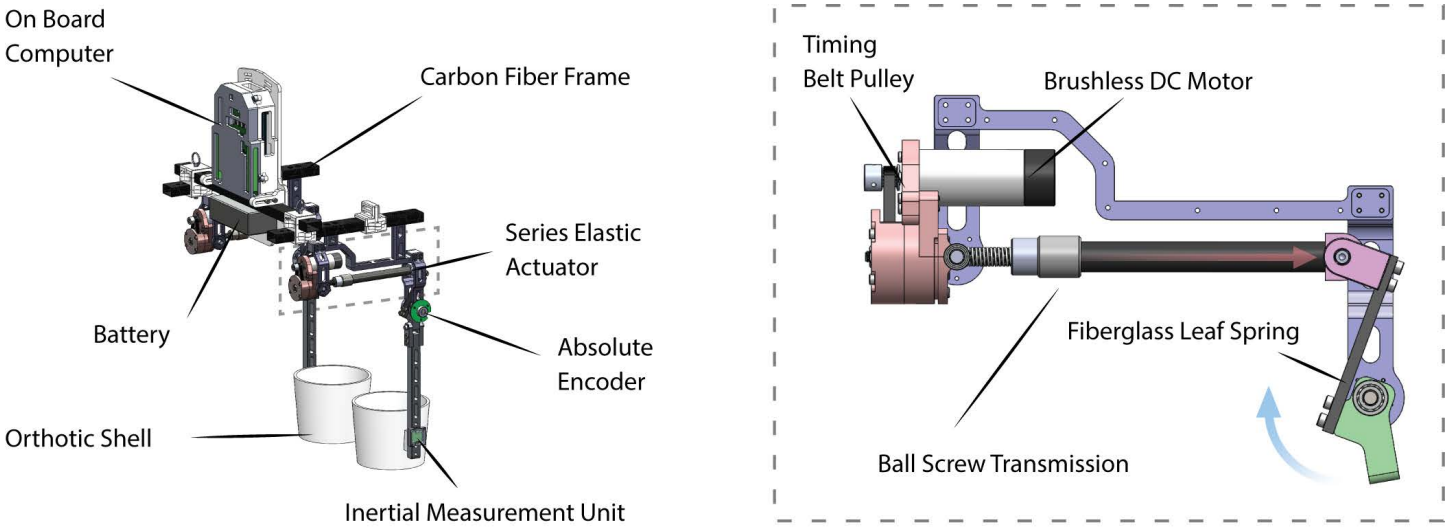

Figure 2. Detailed CAD view of the hip exoskeleton device. Left figure shows the key components in the device. Right figure shows the closed-up view of the series elastic actuator where the red and blue arrows indicate an example of the ball screw travel direction.

Considering an average body weight in the United States, desired specification of the device was calculated with a peak torque of 60 Nm, a maximum continuous torque of 30 Nm, and a maximum velocity of 180 °/sec. This specification ensured that we can assist various levels of torque during normal walking speed. Due to the nature of ball screw transmission having a linear motion with its force being exerted to a moment arm for output torque conversion, reported maximum specifications in torque and velocity are dependent to the hip joint orientation.

1.1 Mechanical Design

SEAs [22] are often used in the robotics field due to its several advantages such as light weight for fine torque measurement, spring working as a low pass filter for any outside disturbance, and reduces output impedance. Several SEAs have been introduced in the literature with often using a planetary gearhead or harmonic drive for speed reducer. Often these planetary gearheads are multi stage which can have negative effect in both actuator weight and back drivability. Back drivability is an important concept in the field of exoskeletons mainly for safety purpose. Having a high back drivability ensures the user to have freedom in moving the leg even when the device is turned off in an emergency situation. A harmonic drive is also a great speed reducer that is often used for its advantage in being near zero backlash in a lightweight package. However, harmonic drives are often expensive and have limitation in only being able to operate at certain input speed range. Ball screw mechanism is advantageous due to its high back drivability and low cost with a lightweight package. Similar concept as [23], a method of linear actuator with carbon fiber tube was used due to its advantage in high strength in axial load (Fig 2). One of the main challenges in applying a ball screw transmission is to make sure the ball screw shaft is well aligned with the carbon fiber actuator tip. The ball screw shaft was fixed in the motor housing (noted as red in Fig. 2) with a double radial bearing while other end of the shaft had a free end for the actuator tip to travel. To minimize the shaft buckling, a PTFE linear bushing, rotating on two flanged radial bearings, was placed at the tip of the ball screw shaft to ensure a proper alignment. Additionally, a pivot joint that the actuator housing rotates about was located at the center line of the ball screw shaft to ensure no moments were transmitted through the actuator. Several materials were used in the literature for spring in the SEA such as steel and titanium [17, 24]. While each materials may have certain advantages, most of them have poor power density. A novel approach of using a fiberglass leaf spring from [25] was utilized for its high energetic storage (up to 8 times per unit mass than spring steel). The study utilized two encoders attached before and after the spring to measure the pure force exerted to the spring. While this method has an advantage of measuring accurate torque at the joint, additional components such as linear guide was needed which may increase the device weight greatly. Instead, the spring was incorporated with a set of strain gauges connected in a full Wheatstone bridge for reading the deflection of the spring. The output hip joint angle was measured with an absolute encoder to ensure both hip joint movement as well as calculation of converting force exerted from a linear motion of ball screw to torque from a rotational motion at the hip joint. Lastly, body orientation in both thighs and the pelvis was measured using a set of inertial measurement units (IMUs).

1.2 Design Architecture

The actuator used a 200W brushless DC motor (EC30, Maxon Motor, Switzerland) rated at 36V for its advantage in having high power to weight ratio (Fig. 3). The motor was equipped with a quadrature incremental encoder and a hall effect sensor operated with a servo driver (ESCON 50/5 Module, Maxon Motor, Switzerland) where both actuators were powered by two 18.5 V lithium polymer battery (Venom Power, USA) connected in series. As the motor had small internal inductance,

Downloaded from http://asmedigitalcollection.asme.org/DSCC/proceedings-pdf/DSCC2018/51890/V001T12A002/2376481/v001t12a002-dscc2018-9198.pdf by Georgia Institute of Technology user on 10 August 2020

Copyright © 2018 ASME

additional inductors were put in series at each phases to mitigate current ripples. The motor drives a 2.5 mm lead length and 10 mm diameter ball screw (Thomson Linear Motion, USA) with an initial timing belt transmission with 2:1 pulley ratio (Misumi, USA). A ball nut is then coupled with a carbon fiber tube with an actuator tip which is connected to a fiberglass leaf spring (Gordon Composites, USA). Fiberglass thickness was simulated with a finite element method with CAD software to analyze the required deflection for strain gauges to have sufficient range of readings while ensuring deflection only occurs within the safe operating range for both spring fracture and strain gauge failure. At both the top and bottom of the fiberglass spring, a set of dual 350 Ω strain gauges (Omega Engineering, USA) were placed to make a full Wheatstone bridge. Full bridge is often preferable over quarter or half bride when using a strain gauge for robotic application as readings tend to drift when the device is operated for long period of time. The strain gauges were calibrated experimentally in both directions with a custom made rig system similar to the hip joint unit of the device by applying different known weights.

A 14-bit resolution absolute magnetic encoder (Orbis, Renishaw, UK) was mounted at the output shaft to measure the hip joint angle. The encoders communicated with the main microprocessor running with SPI communication at 40 MHz. Three inertial measurement units (Micro USB, Yost Labs, USA) were mounted along each thigh shells and by the torso adjacent to the backpack unit for measuring the limb orientation. Each IMU communicated with the microprocessor with UART communication with a baud rate of 115,200 bits/sec. Lastly, a force sensitive resistor was placed at each heel to detect the start of a gait cycle. All of the sensors and motors on the device were

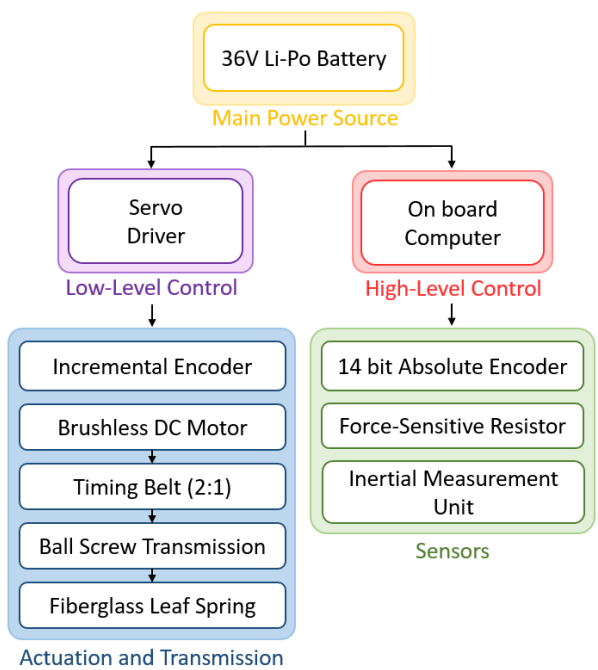

Figure 3. Design architecture of the exoskeleton. Blue box shows the key components used in the series elastic actuator. Main sensors that are used in the device are shown in the green box.

controlled with an on board single board computer (myRIO, National Instruments, USA) equipped with an FPGA chip running the low level closed loop torque control at 200 Hz. All of the sensors were powered from the main battery stepped down to operating voltage with a DC-DC converter.

Torque conversion using the ball screw transmission is critical as it governs the desired torque input at the hip joint (Fig. 4). The actuator rotates about two joints, J_1 and J_2 where J_1 is the output joint and J_2 is the passive joint that the actuator rotates about as ball screw actuator lengthens. As there is an additional linear motion in the transmission system while translating the motor torque to the output joint torque, it is required to calculate the ball screw orientation angle, α, that will be used in converting the linear force to the output torque.

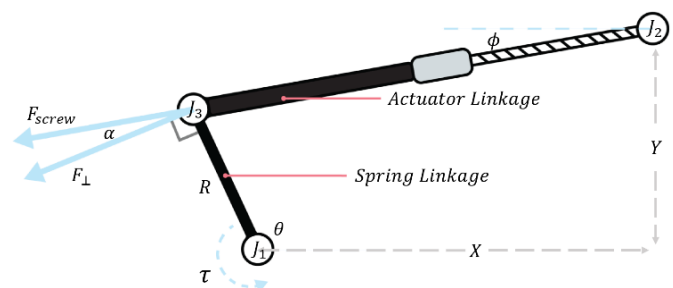

Figure 4. Torque calculation of the ball screw actuator. Blue arrow shows the ball screw actuator travel direction. Ball screw orientation angle, α, is used to convert the force exerted by the actuator to the output torque at the hip joint.

In order to calculate α, two angles θ and ϕ are required where θ is the spring linkage angle and ϕ is the ball screw linkage angle both with respect to the horizontal plane. θ can be measured directly using the absolute encoder while ϕ can be estimated using θ, moment arm length, R, and fixed horizontal and vertical distance between J_1 and J_2 noted as X and Y respectively. Using a basic trigonometry function, horizontal and vertical distance of the actuator tip joint, J_3, can be calculated which can be used to compute ϕ. Complete equation to calculate actuator orientation angle, α, is shown by Eq. 1.

$$\alpha = \frac{\pi}{2} - \left(\theta + \tan^{-1}\left(\frac{X+Rcos\theta}{Y-Rsin\theta}\right)\right) \tag{1}$$

After calculating α, the linear force exerted from the ball screw, F_{screw}, can be converted to the force perpendicular to the spring linkage, $F_\perp$. By using $F_\perp$ multiplied by the moment arm length, R, torque at the output shaft can be calculated for the entire hip joint angle range. The overall equation for converting the input motor torque to output joint torque is shown by Eq. 2, where N is the initial gear ratio of the timing belt pulley, P is the screw lead length, and τ_m is the input motor torque.

$$\tau_{hip} = \frac{2\pi NRcos\alpha}{P}\tau_m \tag{2}$$

Copyright © 2018 ASME

Downloaded from http://asmedigitalcollection.asme.org/DSCC/proceedings-pdf/DSCC2018/51890/V001T12A002/2376481/v001t12a002-dscc2018-9198.pdf by Georgia Institute of Technology user on 10 August 2020

1.3 Controller Design

The device was designed as to be an autonomous hip exoskeleton capable of testing wide variety of controllers. In order to implement different type of controllers to the device, control structure was broken down into three different tiers, high, mid, and low-level layers. Additionally, separating the control layers can aid in implementation of the controller for real time application. For example, the high-level controller will run its state estimation algorithm with a slower sampling rate in microprocessor whereas the low-level controller will run its loop faster in the FPGA chip with a more deterministic manner. High-level control layer is set for implementing a state estimation task where it understands what state the user is in such as walking, sitting, and climbing stairs and ramps [26]. Another important aspect in the high-level layer is to have an algorithm that updates the user's state in terms of gait cycle. This algorithm is important as gait cycle dictates when to provide assistance to the user. A common method in the literature utilizes a simple finite state machine by discretizing the gait cycle into different state such as stance and swing [27]. Although this approach may be easy to incorporate to the control layer, it limits the variation of continuously assisting the user in different point in the gait cycle. Study done in [19] has shown that onset timing of assistance is critical in achieving the best energetic benefits. To accommodate with more flexibility in providing correct assistance, the device utilized a continuous gait phase estimator that would predict the user's gait cycle in terms of percentage. For the mid-level layer, different controllers can be implemented using a set of dynamic equations to convert the user input to output torque. Several controllers had been introduced for human augmentation robotics in the literature such as impedance, EMG, and torque controller [28-30]. Torque controller has a big advantage as different type of torque profile can be generated depending on the application while maintaining simplicity in overall. Several exoskeletons have shown positive results using a torque controller [14, 31]. After understanding the user's gait phase from the high-level layer, torque controller in mid-level layer generates a torque profile with a desired magnitude and timing as an input command to the low-level layer. Lastly, low-level layer incorporates the commanded current input in a closed loop torque control utilizing the spring deflection reading from the strain gauges with closed loop PID control.

High-Level Control

Gait phase is a continuous variable that ranges from 0% to 100% over a gait cycle. The device utilizes a set of FSR sensors to detect the heel contact of the user. While the FSR sensor is often prone to high noise, as the sensor was used as an event marker, raw FSR signals didn't affect the gait estimation. Each stride time (time over each gait cycle) was measured using the heel contact happening with FSR sensor reading and was averaged over the most recent 5 strides. Time since the current heel strike was then normalized to the average stride time to estimate the current gait phase. Although this algorithm has an advantage of estimating the gait phase correctly while not adding complexity the device, it has limitation of not being able to respond to the change of walking speed fast. It will take 5 additional gait strides until the average stride time adapts to new speed. A more robust gait phase estimator utilizing different mechanical sensors on board (such as encoders and IMUs) for gait phase estimation may be beneficial but for the purpose of this study, proposed gait phase estimator was sufficient enough to validate the device performance.

Mid-Level Control

As mentioned above, the advantage of using the torque controller is its simplicity while having various control over different torque profile. As the robot interacts with the human directly, it had be assured that the assistance does not exert torque in an impulse manner such as a step input. This can cause high discomfort to the user when the assistance magnitude is high. Instead, the assistance profile was preset with a trapezoidal profile where the torque ramps up to and down from the desired magnitude. The conventional method in generating the assistance profile is through a parabola shape with the desired torque being the vertex. However, this approach has limitation because desired torque command is only achieved for short amount of time period. The proposed trapezoidal method has an advantage of ensuring that the desired torque is held constantly throughout the assistance region of the gait cycle.

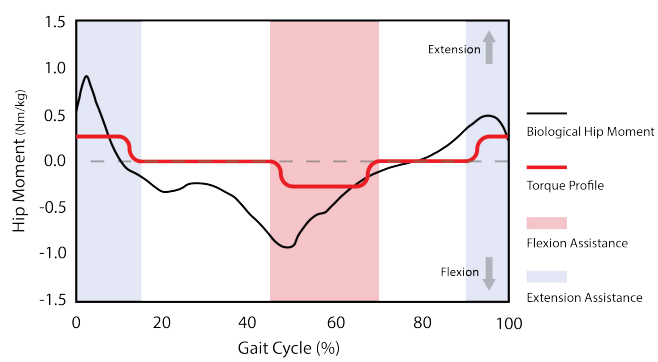

Figure 5. Example of torque assistance profile during walking. Red and blue regions indicate the hip flexion and extension assistance area respectively. Torque assistance profile (shown as red line) is generated with a desired onset timing and magnitude where onset timing was optimized at 45% and 90% for hip flexion and extension [19].

The gait cycle composed a hip flexion and extension assistance region where the onset assistance timing were 45% and 90% of the gait cycle respectively (Fig. 5). These timing variables were optimized based on our previous work with hip exoskeletons [19]. Note that during the phase when there is no assistance, command is zero torque. This mode is called zero impedance, a mode where the device only follows with the user's leg movement by moving in the direction that the torque is being measured. While high back drivability using a ball screw transmission greatly reduces the output inertia, walking at fast pace greatly impedes the user due to the device weight and friction. Zero impedance mode compensates this phenomenon

Downloaded from http://asmedigitalcollection.asme.org/DSCC/proceedings-pdf/DSCC2018/51890/V001T12A002/2376481/v001t12a002-dscc2018-9198.pdf by Georgia Institute of Technology user on 10 August 2020

Copyright © 2018 ASME

by providing an equal torque that is being measured during movement to ensure the interaction torque between the user and the exoskeleton is zero.

Low-Level Control

Low-level layer intakes the torque command in a form of current command (Fig. 6). This current command is converted to a PWM signal mapped into a form of duty cycle with a frequency of 2 kHz. Additional digital commands in the servo drive was used to enable and control the direction of the motor. The strain gauge reading measures the output torque with a deflection of the fiberglass leaf spring. This torque was converted using both strain gauge readings and ball screw orientation angle calculated with the hip joint angle measured from the encoder. To minimize the high frequency noise of the raw signal, 200 Hz first order Butterworth low pass filter was implemented. While the device used proper filtering to minimize any possible signal attenuation, nature of analog sensor readings included additional noise in the strain gauge readings. For example, using a power supply in a benchtop setting caused a 60 Hz power line hum which cannot be filtered out with 200 Hz low pass filter. For such situation, proper grounding was done in the custom circuit board. A simple PID control was used for a closed loop torque control. Integral gain was not used as significance of stead state error was marginal in our application. Proportional and derivative gains were tuned experimentally with a conventional step response test with a desired rise time and settling time. The gains were tuned to have similar response in both flexion and extension direction to guarantee similar actuator response can be achieved.

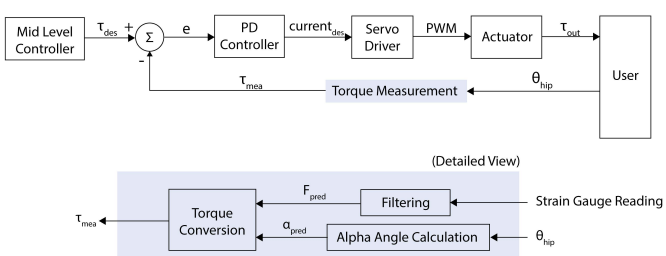

Figure 6. Low-level control flow chart of the device. Low-level closed loop torque control utilizes PD control. Blue box is shown for detailed illustration of the output torque measurement.

2 DEVICE VALIDATION

The key part in evaluating the device performance was to validate the closed loop torque control. While achieving the desired torque is important, the torque bandwidth was also critical as this relates to the device response in changing the command input. Bandwidth plays a critical role when the device is in a zero impedance mode during walking. This may not be as critical at standing or slow movement but may be critical when walking at fast pace. A set of benchtop testing was done to first validate the torque response of the device to ensure low-level control gains are properly tuned. After, the device was tested on five different able bodied subjects walking on a treadmill at constant speed. During walking, subjects were assisted with a biological torque profile with desired magnitude and onset timing for both hip flexion and extension.

2.1 Methods

Benchtop Testing

Benchtop testing of the device was conducted with the exoskeleton leg fixed at a certain position with a mechanical hard stop. Different levels of torque step input in both flexion and extension directions were commanded. As the device utilizes a linear actuator, step response of the torque command were required to show similar results in both directions. By observing the output torque measured from the spring, both proportional and derivative gains were tuned. During the gains tuning process, filter frequency of the strain gauge reading were also observed to check if there is any significant attenuation of the signal. After the step response testing, interaction torque of the device at zero impedance mode was observed. Output torque was observed while back driving the leg with the controller commanding zero interaction torque. The leg was moved in a certain fashion with a form of pseudo sinewave with approximately 5 Hz bandwidth in both flexion and extension direction. Also, this interaction torque during zero impedance mode will approximate how much impedance will the subject experiences during walking with the exoskeleton.

Human Subject Testing

After the exoskeleton had been validated in benchtop settings, the device was tested on able bodied subjects to validate the device performance in providing assistance during walking. The study was approved by the Georgia Institute of Technology Institutional Review Board, and informed written consent was obtained from all subjects. Five healthy subjects (four males and one female) with age range from 21 to 27 years, height range from 165 cm to 178 cm, and body mass range from 60 kg to 81 kg were recruited (Table 2).

Table 2. Subject Information

Subject	Sex	Age	Weight (kg)	Height (m)
1	M	23	70	1.78
2	M	27	78	1.73
3	M	21	72	1.73
4	M	21	81	1.75
5	F	24	60	1.65
Average ± SD		23.2 ± 2.5	72.2 ± 8.1	1.73 ± 0.05

Subjects attended two sessions where the first visit was conducted as a training session and second visit was used to collect the data. During the first session, the device was adjusted to ensure proper fitting especially to make sure that the device hip joint is aligned with the subject's biological hip joint. After the fitting, the subject walked on the device starting with zero impedance mode to slowly adapt to walking in the device. Lastly, different magnitudes of torque were provided in both hip flexion and extension to give the user time to accommodate to the

Downloaded from http://asmedigitalcollection.asme.org/DSCC/proceedings-pdf/DSCC2018/51890/V001T12A002/2376481/v001t12a002-dscc2018-9198.pdf by Georgia Institute of Technology user on 10 August 2020

Copyright © 2018 ASME

device. Unlike many previous studies, there were no user specific tuning parameters in the controller.

During the second visit, subjects walked with different levels of torque assistance while walking at 0.8 m/s on a treadmill (TuffTread, USA) for 6 minutes. Torque assistance levels were normalized to able bodied biological peak torque at the hip joint during 0.8 m/s walking speed which is 0.5 Nm/kg [32] for both flexion and extension. Three different assistance levels, 13%, 26%, and 40% of the peak biological hip torque were tested during walking for both hip flexion and extension. During the human testing, data from FSR sensor, encoders, and strain gauge reading on the device were recorded. FSR sensor data was used for segmenting the data into every gait cycle. Encoder values were analyzed to observe the hip joint kinematics over different assistance condition. Lastly, measured output torque from the strain gauges were compared to desired torque command to validate torque tracking of the device.

2.2 Results

Benchtop Testing Results

For different levels of torque command, both flexion and extension direction were tested to tune the proportional and derivative gain of the low-level control (Fig. 7). An initial 2 Nm of torque was applied against the mechanical hard stop to mitigate any backlash. Total of 5 Nm, 10 Nm, and 15 Nm were applied in both directions. As shown in the graph, while a low torque step input had a fairly damped response, a higher torque command had an increase of initial overshoot for about 15% of commanded input. Rise time of the step response was approximately 10 ms, 20 ms. and 30 ms for 3 different levels of torque input respectively.

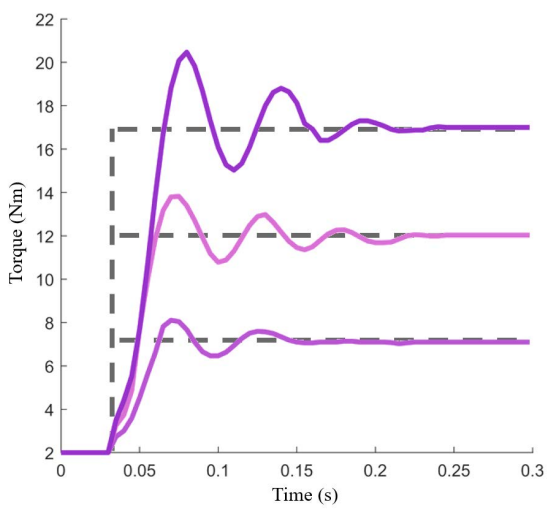

Figure 7. Step response result of the exoskeleton. Plotted results represent the torque step response of the device in flexion direction. Dashed lines indicate the different levels of desired torque step input.

The device interaction torque was tested with different frequencies by back driving the device leg while putting the controller into zero impedance mode (Fig. 8). A pseudo sinewave was generated manually with a 20° range of motion in both directions. As shown in the figure, increase in the movement of the leg increases the measured output torque. The motion was repeated with approximately 5 Hz frequency to observe the interaction torque which was measured to be around a maximum of 4 Nm. While this result represents that there will still be residual impedance occurring at movement with higher frequencies, magnitudes of torque that is experienced are in reasonable range and can be tolerable.

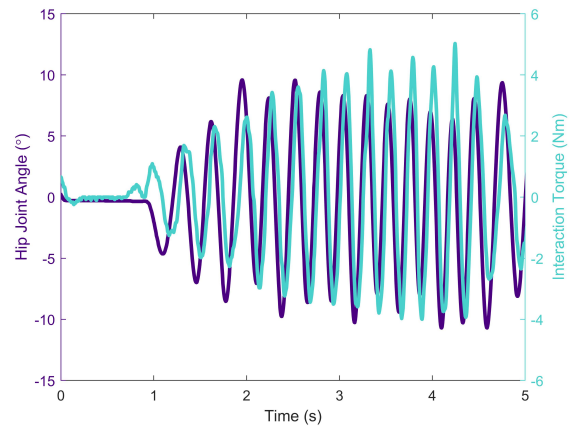

Figure 8. Interaction torque response of the exoskeleton. Output interaction torque is plotted while exoskeleton leg was back driven with certain frequency (approximately 5 Hz). The result will illustrate the impedance that the user will experience during walking on the device in zero impedance mode.

Human Subject Testing Results

The hip joint kinematic results of a subject walking on the exoskeleton device at different assistance condition was compared with the literature data [21]. Overall, at the zero impedance mode, the result showed that the device did not change the user's gait pattern (Fig. 9). It is important to ensure that the joint kinematics of the user does not change as it may

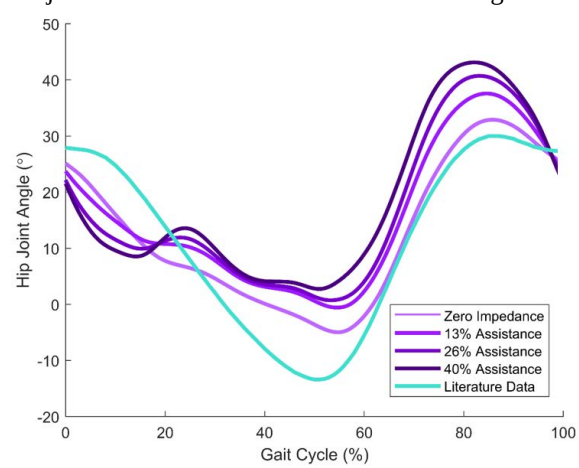

Figure 9. Hip joint kinematics while walking on the exoskeleton with different assistance levels. Different purple color graphs indicate different assistance levels. Blue graph was plotted as a reference to show the human hip joint kinematics without the exoskeleton during walking [21].

Copyright © 2018 ASME

Downloaded from http://asmedigitalcollection.asme.org/DSCC/proceedings-pdf/DSCC2018/51890/V001T12A002/2376481/v001t12a002-dscc2018-9198.pdf by Georgia Institute of Technology user on 10 August 2020

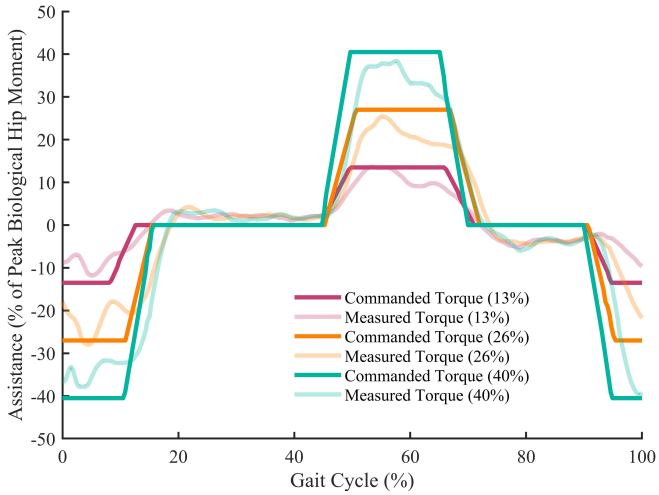

Figure 10. Torque tracking of the exoskeleton during walking at the three different assistance levels corresponding to 13%, 26%, and 40% of peak biological torque (Subject 2). Flexion and extension assistance were provided at 45% and 90% of the gait cycle respectively for duration of 25% window length. Solid lines represent the commanded input torque and transparent lines with corresponding color represent the measured output torque.

induce higher energetic cost during walking. As shown in the figure, different levels of assistance changed the user's gait pattern by increasing the hip flexion range. Also, increase of assistance level decreased hip extension.

Three different levels of desired torque command for hip flexion and extension were provided correctly at desired onset timing (Fig. 10). For all assistance conditions across all subjects, the onset timing for both flexion and extension had an average error of less than 1%. It was validated that the gait phase estimator worked correctly and the torque assistance was provided at desired onset timing. Generally, results across all five subjects showed a similar trend in torque tracking where extension torque tracking had better performance than flexion region. For example, during the flexion assistance region (45% to 70%) measured output showed a drop in torque prior to the end of flexion assistance. Lastly, even though absolute magnitude of assistance level is within the range of interaction torque (Fig. 8), lower torque assistance (13%) showed relatively good torque tracking as the other assistance conditions.

3 DISCUSSION

We found that subjects increased hip flexion and decreased hip extension during walking with different levels of assistance. However, hip range of motion stayed consistent. This phenomenon of underlying dynamic of human gait being modified with the powered exoskeleton is often observed where user tends to have a marching gait pattern when assistance is provided. This gait pattern was shown consistent across all five subjects. Generally, such gait pattern makes the user take shorter steps. While the effect of taking shorter steps to the user was not validated in this study, we will further investigate by observing the user's metabolic cost with increase of assistance can explain the result of kinematic change in human energetics.

Extension torque had better performance in torque tracking than flexion assistance (Fig. 10). This may be due to faster leg movement caused at the hip joint during flexion where the user is driving the device rather that the device providing assistance which shows reduced measured output torque in overall. Also, this phenomenon may be caused due to the user walking on a treadmill. Mainly, the extension assistance is provided during the stance phase where the user's foot is in contact with the ground moving at a constant speed. The device can exert better torque to the leg with this situation as leg is moving in a more constant speed whereas hip flexion can have higher variance (such as acceleration and deceleration) in movement depending on the user as the leg is in the air. Additionally, torque tracking result may be different than the result from the benchtop testing due to the actuator applying a torque to the limb rather than to a rigid hard stop. Soft tissue of the human body dampens and partially absorbs the device assistance. Thus, torque tracking result shows slight delay (or phase shift) in readings as the device needs to overcome this tissue dampening to fully assist the user through body's skeletal structure.

As shown with the human subject testing results, our gait phase estimator was able to accurately estimate the user's gait phase in real time to provide assistance at desired onset timing. One of the main limitations in proposed gait phase estimator is not being able to adapt to changes in walking speed. During a constant walking speed, user may often change the stride frequencies. As the gait phase estimator base the normalization with 5 previous gait cycle, change in stride frequency and/or walking speed takes in effect after certain number of steps. This aspect may be a limitation if the device is walked over ground-level. While current gait phase estimator performed well for proposed test setting, more robust algorithm for estimating gait phase such as machine learning approach using different sensors on the device may be introduced in the future to be more adaptable to various movements.

While our exoskeleton has several structural advantages such as being able to provide high torque to the user than the other exoskeletons that are currently studied in the field [14, 15], it has a main limitation in overall device weight. Mainly, this weight came from both frame structure and the orthotic interface where both of them were initially designed to withstand any structural vibrations during high torque assistance. This is an important aspect to keep in consideration as some dynamic movements from the user such as lateral pelvic motion may cause misalignment and torsion of the device along the frontal plane. This phenomenon can not only induce device failure mechanically, but also cause incorrect reading at the strain gauge. Having a more rigid structure in both actuator frame and orthotic interface allowed to withstand these vibrations. However, additional iteration of design modification in the device interface may further reduce the overall weight. Further research and engineering development of the device may open a broader impact of this device to be used in a clinical population or elderly where the assistance at the hip joint can be benefitted with a greater amount.

Downloaded from http://asmedigitalcollection.asme.org/DSCC/proceedings-pdf/DSCC2018/51890/V001T12A002/2376481/v001t12a002-dscc2018-9198.pdf by Georgia Institute of Technology user on 10 August 2020

Copyright © 2018 ASME

4 CONCLUSION

Our hip exoskeleton device assists users by providing mechanical power at the hip joint during human walking. The device utilizes a SEA which allows a more robust interaction between the device and the user and ensures that the assistance is being provided accurately at the output joint. The device demonstrated its capability in implementing different type of control algorithms such as EMG control that may be more innovative approach.

ACKNOWLEDGMENT

The authors thank Dr. Geza Kogler for insights in designing orthotic interface, Claire Kilpatrick and Seung Eun Lee for helping out fabricating the interface, and Joonho Seo for helping with the initial design. We acknowledge Courtland Bivens and Michael Mayo at GTRI for their contributions and GTRI IRAD funding. Additionally, this work was funded by a seed grant through the Institute for Robotics and Intelligent Machines (IRIM) at Georgia Tech.

REFERENCES

[1] H. Hodson. (2014) Robotic suit gives shipyard workers super strength. *New Scientist*.

[2] H. Yu, I. S. Choi, K.-L. Han, J. Y. Choi, G. Chung, and J. Suh, "Development of a upper-limb exoskeleton robot for refractory construction," *Control Engineering Practice*, vol. 72, pp. 104-113, 2018/03/01/ 2018.

[3] A. B. Zoss, H. Kazerooni, and A. Chu, "Biomechanical design of the Berkeley lower extremity exoskeleton (BLEEX)," *IEEE/ASME Transactions on Mechatronics*, vol. 11, no. 2, pp. 128-138, 2006.

[4] K. N. Gregorczyk, L. Hasselquist, J. M. Schiffman, C. K. Bensel, J. P. Obusek, and D. J. Gutekunst, "Effects of a lower-body exoskeleton device on metabolic cost and gait biomechanics during load carriage," *Ergonomics*, vol. 53, no. 10, pp. 1263-1275, 2010.

[5] S. Jezernik, G. Colombo, T. Keller, H. Frueh, and M. Morari, "Robotic Orthosis Lokomat: A Rehabilitation and Research Tool," *Neuromodulation: Technology at the Neural Interface*, vol. 6, no. 2, pp. 108-115, 2003.

[6] M. Sczesny-Kaiser *et al.*, "Neurorehabilitation in chronic paraplegic patients with the HAL® exoskeleton–preliminary electrophysiological and fMRI data of a pilot study," in *Converging Clinical and Engineering Research on Neurorehabilitation*: Springer, 2013, pp. 611-615.

[7] R. J. Farris, H. A. Quintero, S. A. Murray, K. H. Ha, C. Hartigan, and M. Goldfarb, "A preliminary assessment of legged mobility provided by a lower limb exoskeleton for persons with paraplegia," *IEEE Transactions on Neural Systems and Rehabilitation Engineering*, vol. 22, no. 3, pp. 482-490, 2014.

[8] G. Zeilig, H. Weingarden, M. Zwecker, I. Dudkiewicz, A. Bloch, and A. Esquenazi, "Safety and tolerance of the ReWalk™ exoskeleton suit for ambulation by people with complete spinal cord injury: A pilot study," *The Journal of Spinal Cord Medicine*, vol. 35, no. 2, pp. 101-96, 2012.

[9] S. A. Kolakowsky-Hayner, J. Crew, S. Moran, and A. Shah, "Safety and feasibility of using the EksoTM bionic exoskeleton to aid ambulation after spinal cord injury," *Journal of Spine*, 2013.

[10] G. S. Sawicki, C. L. Lewis, and D. P. Ferris, "It pays to have a spring in your step," *Exercise and sport sciences reviews*, vol. 37, no. 3, p. 130, 2009.

[11] B. R. Umberger and J. Rubenson, "Understanding muscle energetics in locomotion: new modeling and experimental approaches," *Exercise and sport sciences reviews*, vol. 39, no. 2, pp. 59-67, 2011.

[12] R. R. Neptune, C. P. McGowan, and S. A. Kautz, "Forward dynamics simulations provide insight into muscle mechanical work during human locomotion," *Exercise and sport sciences reviews*, vol. 37, no. 4, p. 203, 2009.

[13] R. C. Browning, J. R. Modica, R. Kram, and A. Goswami, "The effects of adding mass to the legs on the energetics and biomechanics of walking," *Med Sci Sports Exerc*, vol. 39, no. 3, pp. 515-25, Mar 2007.

[14] F. Giovacchini *et al.*, "A light-weight active orthosis for hip movement assistance," *Robotics and Autonomous Systems*, 2014.

[15] A. T. Asbeck, K. Schmidt, and C. J. Walsh, "Soft exosuit for hip assistance," *Robotics and Autonomous Systems*, vol. 73, pp. 102-110, 2015/11/01/ 2015.

[16] K. Seo, J. Lee, Y. Lee, T. Ha, and Y. Shim, "Fully Autonomous Hip Exoskeleton Saves Metabolic Cost of Walking," (in English), *2016 Ieee International Conference on Robotics and Automation (Icra)*, pp. 4628-4635, 2016.

[17] T. Zhang, M. Tran, and H. Huang, "Design and Experimental Verification of Hip Exoskeleton With Balance Capacities for Walking Assistance," *IEEE/ASME Transactions on Mechatronics*, vol. 23, no. 1, pp. 274-285, 2018.

[18] Y. Kusuda, "In quest of mobility–Honda to develop walking assist devices," *Industrial Robot: An International Journal*, vol. 36, no. 6, pp. 537-539, 2009.

[19] A. J. Young, J. Foss, H. Gannon, and D. P. Ferris, "Influence of Power Delivery Timing on the Energetics and Biomechanics of Humans Wearing a Hip Exoskeleton," *Front Bioeng Biotechnol*, vol. 5, p. 4, 2017.

[20] National Center for Health Statistics (U.S.) and National Health and Nutrition Examination Survey (U.S.), *Anthropometric reference data for children and adults : United States, 2011-2014* (Vital and health statistics Series 3, Data from the National Health and Nutrition Examination Survey, no. number 39). Hyattsville, Maryland: U.S. Department of Health and Human Services, Centers for Disease Control and Prevention, National Center for Health Statistics, 2016, p. p.

Downloaded from http://asmedigitalcollection.asme.org/DSCC/proceedings-pdf/DSCC2018/51890/V001T12A002/2376481/v001t12a002-dscc2018-9198.pdf by Georgia Institute of Technology user on 10 August 2020

Copyright © 2018 ASME

[21] D. Winter, J. Eng, and M. Ischac, "Three-dimensional moments, powers and work in normal gait: implications for clinical assessments," in *Human motion analysis: current applications and future directions*, G. Harris and S. PA, Eds. New York: IEEE Press, 1996.

[22] J. Pratt, B. Krupp, and C. Morse, "Series elastic actuators for high fidelity force control," *Industrial Robot: An International Journal*, vol. 29, no. 3, pp. 234-241, 2002.

[23] C. Knabe *et al.*, "Design of a Series Elastic Humanoid for the DARPA Robotics Challenge," (in English), *2015 Ieee-Ras 15th International Conference on Humanoid Robots (Humanoids)*, pp. 738-743, 2015.

[24] N. Paine, S. Oh, and L. Sentis, "Design and Control Considerations for High-Performance Series Elastic Actuators," *IEEE/ASME Transactions on Mechatronics*, vol. 19, no. 3, pp. 1080-1091, 2014.

[25] M. K. Shepherd and E. J. Rouse, "Design and Validation of a Torque-Controllable Knee Exoskeleton for Sit-to-Stand Assistance," (in English), *Ieee-Asme Transactions on Mechatronics*, vol. 22, no. 4, pp. 1695-1704, Aug 2017.

[26] A. Young, A. Simon, N. Fey, and L. Hargrove, "Intent Recognition in a Powered Lower Limb Prosthesis using Time History Information," *Annals of Biomedical Engineering*, 2013.

[27] H. A. Quintero, R. J. Farris, and M. Goldfarb, "A method for the autonomous control of lower limb exoskeletons for persons with paraplegia," *Journal of Medical Devices*, vol. 6, no. 4, p. 041003, 2012.

[28] J. A. Blaya and H. Herr, "Adaptive control of a variable-impedance ankle-foot orthosis to assist drop-foot gait," *IEEE Transactions on Neural Systems and Rehabilitation Engineering*, vol. 12, no. 1, pp. 24-31, 2004.

[29] L. Mooney, E. Rouse, and H. Herr, "Autonomous exoskeleton reduces metabolic cost of human walking during load carriage," *Journal of NeuroEngineering and Rehabilitation*, vol. 11, no. 1, p. 80, 2014.

[30] A. J. Young, H. Gannon, and D. P. Ferris, "A Biomechanical Comparison of Proportional Electromyography Control to Biological Torque Control Using a Powered Hip Exoskeleton," *Frontiers in Bioengineering and Biotechnology*, 10.3389/fbioe.2017.00037 vol. 5, p. 37, 2017.

[31] B. T. Quinlivan *et al.*, "Assistance magnitude versus metabolic cost reductions for a tethered multiarticular soft exosuit," *Science Robotics*, 10.1126/scirobotics.aah4416 vol. 2, no. 2, 2017.

[32] K. E. Zelik and A. D. Kuo, "Human walking isn't all hard work: evidence of soft tissue contributions to energy dissipation and return," *The Journal of experimental biology*, vol. 213, no. 24, pp. 4257-4264, 2010.

Downloaded from http://asmedigitalcollection.asme.org/DSCC/proceedings-pdf/DSCC2018/51890/V001T12A002/2376481/v001t12a002-dscc2018-9198.pdf by Georgia Institute of Technology user on 10 August 2020

Copyright © 2018 ASME